THE JOURNAL OF BIOLOGICAL CHEMISTRY VOL. 282, NO. 20, pp. 14708–14718, May 18, 2007


# Interaction of the Mitochondria-targeted Antioxidant MitoQ with Phospholipid Bilayers and Ubiquinone Oxidoreductases*[S]

Received for publication, December 14, 2006, and in revised form, February 27, 2007 Published, JBC Papers in Press, March 16, 2007, DOI 10.1074/jbc.M611463200

**Andrew M. James[‡], Mark S. Sharpley[‡], Abdul-Rahman B. Manas[§], Frank E. Frerman[¶], Judy Hirst[‡], Robin A. J. Smith[§], and Michael P. Murphy [‡1]**

*From the [‡]Medical Research Council Dunn Human Nutrition Unit, Wellcome Trust/MRC Building, Hills Road, Cambridge CB2 2XY, United Kingdom, the [¶]Departments of Pediatrics and Pharmaceutical Sciences, University of Colorado Health Sciences Center, Denver, Colorado 80262, and the [§]Department of Chemistry, University of Otago, P. O. Box 56, Dunedin 9001, New Zealand*

**$MitoQ_{10}$ is a ubiquinone that accumulates within mitochondria driven by a conjugated lipophilic triphenylphosphonium cation ($TPP^+$). Once there, $MitoQ_{10}$ is reduced to its active ubiquinol form, which has been used to prevent mitochondrial oxidative damage and to infer the involvement of reactive oxygen species in signaling pathways. Here we show $MitoQ_{10}$ is effectively reduced by complex II, but is a poor substrate for complex I, complex III, and electron-transferring flavoprotein (ETF):quinone oxidoreductase (ETF-QOR). This differential reactivity could be explained if the bulky $TPP^+$ moiety sterically hindered access of the ubiquinone group to enzyme active sites with a long, narrow access channel. Using a combination of molecular modeling and an uncharged analog of $MitoQ_{10}$ with similar sterics ($tritylQ_{10}$), we infer that the interaction of $MitoQ_{10}$ with complex I and ETF-QOR, but not complex III, is inhibited by its bulky $TPP^+$ moiety. To explain its lack of reactivity with complex III we show that the $TPP^+$ moiety of $MitoQ_{10}$ is ineffective at quenching pyrene fluorophors deeply buried within phospholipid bilayers and thus is positioned near the membrane surface. This superficial position of the $TPP^+$ moiety, as well as the low solubility of $MitoQ_{10}$ in non-polar organic solvents, suggests that the concentration of the entire $MitoQ_{10}$ molecule in the membrane core is very limited. As overlaying $MitoQ_{10}$ onto the structure of complex III indicates that $MitoQ_{10}$ cannot react with complex III without its $TPP^+$ moiety entering the low dielectric of the membrane core, we conclude that the $TPP^+$ moiety does anchor the tethered ubiquinol group out of reach of the active site(s) of complex III, thus explaining its slow oxidation. In contrast the ubiquinone moiety of $MitoQ_{10}$ is able to quench fluorophors deep within the membrane core, indicating a high concentration of the ubiquinone moiety within the membrane and explaining its good antioxidant efficacy. These findings will facilitate the rational design of future mitochondria-targeted molecules.**

The mitochondria-targeted antioxidant $MitoQ_{10}$ comprises a triphenylphosphonium cation ($TPP^+$)[2] attached to a ubiquinone moiety by a saturated 10-carbon chain (1). The lipophilic cation leads to the extensive accumulation of $MitoQ_{10}$ within mitochondria where the ubiquinone is reduced to its active antioxidant ubiquinol form (1–3). Accumulation and subsequent reduction of $MitoQ_{10}$ leads to protection against mitochondrial oxidative damage in a number of *in vitro* and *in vivo* systems (4–7). As $MitoQ_{10}$ is thought to act primarily in the membrane phase by preventing lipid peroxidation (1–3), we attempted to optimize its efficacy by varying the length of the alkyl chain linking the $TPP^+$ and ubiquinone moieties ($MitoQ_n$, $n = 3, 5, 10$, and 15). With these analogs we observed a positive correlation between alkyl chain length and antioxidant efficacy (2) and between alkyl chain length and reduction to its antioxidant ubiquinol form by complex II (3). Furthermore, some oxidoreductases failed to react with any of the MitoQ analogs at an appreciable level (3). To infer the principal sites of reduction of $MitoQ_{10}$ to its antioxidant form within mitochondria, we measured the activity of $MitoQ_{10}$ with isolated complex I, complex II, and electron-transferring flavoprotein (ETF):quinone oxidoreductase (ETF-QOR). Here we show that $MitoQ_{10}$ is rapidly reduced by isolated complex II, but is not a good substrate for isolated ETF-QOR or complex I.

Whereas the greater hydrophobicity of the longer MitoQ analogs would have increased their partitioning into the lipid phase where they would be most available for reduction by dehydrogenases and protective against lipid peroxidation (2, 3), differences in how MitoQ reacted with individual ubiquinone oxidoreductases suggested two additional factors arising from the size and the charge of its $TPP^+$ moiety (3). The $TPP^+$ group of MitoQ is somewhat bulkier than the ubiquinone moiety raising the possibility of sterically hindered access to the active sites

* This work was supported in part by the Medical Research Council, the Foundation for Research, Science and Technology New Zealand, and by Antipodean Biotechnology. The costs of publication of this article were defrayed in part by the payment of page charges. This article must therefore be hereby marked "*advertisement*" in accordance with 18 U.S.C. Section 1734 solely to indicate this fact.

[S] The on-line version of this article (available at http://www.jbc.org) contains supplemental Figs. S1–S3.

[1] To whom correspondence should be addressed: Medical Research Council Dunn Human Nutrition Unit, Wellcome Trust/MRC Bldg., Hills Road, Cambridge CB2 2XY, UK. Tel.: 44-1223-252900; Fax: 44-1223-252905; E-mail: mpm@mrc-dunn.cam.ac.uk.

[2] The abbreviations used are: $TPP^+$, triphenylphosphonium cation; BHM, bovine heart mitochondrial membranes; CHAPS, 3-[(3-cholamidoproyl) dimethylammonio]-1-propane-sulfonate; $CoQ_{1-10}$, ubiquinone with a tail of 1–10 isoprenoid units (2,3-dimethoxy-5-methyl-6-polyprenyl-1,4-benzoquinone); cyt *c*, cytochrome *c*; ETF, electron-transferring flavoprotein; ETF-QOR, electron-transferring flavoprotein:quinone oxidoreductase; MCAD, medium-chain acyl-CoA dehydrogenase; MitoQ, ubiquinone linked to a triphenylphosphonium cation by an alkyl chain of unspecified length; $MitoQ_n$, ubiquinone linked to a triphenylphosphonium cation by an alkyl chain of *n* methylene groups; PC, phosphatidylcholine; $Pyr_n$, pyrene linked to a carboxylic acid by an alkyl chain of *n*-1 methylene groups; SUV, small unilamellar vesicle; SV, Stern-Volmer constant; $TPB^-$, tetraphenylborate anion; TPMP, methyltriphenylphosphonium cation; $\epsilon_r$, relative dielectric constant.

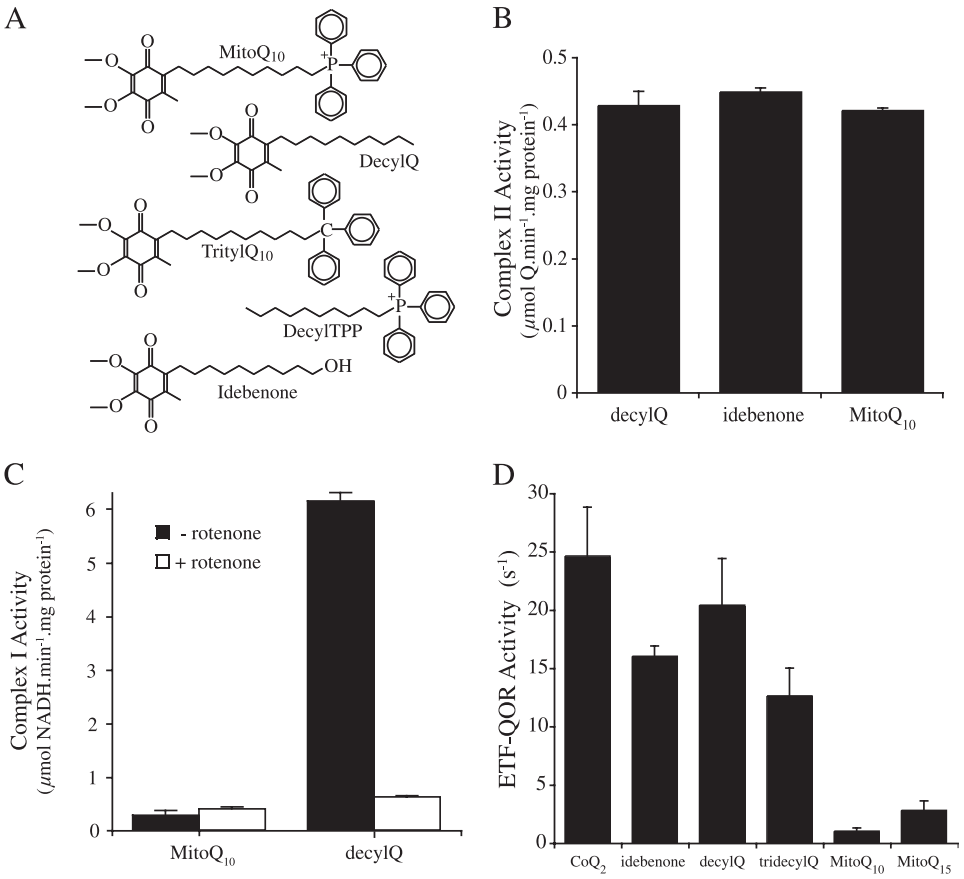


FIGURE 1. **MitoQ$_{10}$ is reduced by isolated complex II but not by isolated ETF-QOR or complex I.** *A*, structures of various ubiquinone and TPP$^+$-containing molecules. *B*, MitoQ$_{10}$ is reduced by isolated complex II. Isolated complex II (~10 $\mu$g protein·ml$^{-1}$) was added to buffer containing 5 mM succinate, asolectin, CHAPS, and 50 $\mu$M of either decylQ, idebenone or MitoQ$_{10}$. The reaction was monitored as the decrease in absorbance at 275 nm due to ubiquinone reduction and this was completely inhibited by 20 mM malonate. Data are the means ± S.D. of three independent experiments. *C*, isolated complex I in the presence of MitoQ$_{10}$ does not oxidize NADH in a rotenone-sensitive manner. Isolated complex I (~2 $\mu$g protein·ml$^{-1}$) was added to buffer containing NADH, asolectin, CHAPS, and 200 $\mu$M of either MitoQ$_{10}$ or decylQ in the presence or absence of rotenone. The reaction was monitored as the decrease in absorbance at 340 nm due to NADH oxidation. Data are the means ± S.D. or range of 2–4 independent experiments. *D*, MitoQ$_{10}$ is a poor substrate for electron-transferring flavoprotein (ETF):quinone oxidoreductase (ETF-QOR). ETF-QOR was added to buffer containing MCAD, ETF, octanoyl-CoA, CHAPS, and 60 $\mu$M of either CoQ$_2$, decylQ, idebenone, tridecylQ, MitoQ$_{10}$, or MitoQ$_{15}$. The reaction was monitored as the decrease in absorbance at 275 nm due to ubiquinone reduction. Data are the means ± S.D.

of some mitochondrial ubiquinone oxidoreductases. Using a sterically similar analog of MitoQ$_{10}$ in which the positively charged phosphonium is replaced with a neutral carbon (tritylQ$_{10}$; Fig. 1*A*), we show that bulkiness of the TPP$^+$ moiety is likely to diminish MitoQ$_{10}$ reduction by complex I.

However, bulkiness does not contribute to the poor oxidation of the reduced form of MitoQ$_{10}$ by complex III. We believed this could be explained by the complicated interaction of relatively hydrophilic TPP$^+$ derivatives, such as the methyltriphenylphosphonium cation (TPMP$^+$), with phospholipid bilayers (8). Numerous studies have led to the following model for the passage of such lipophilic cations through membranes (9–13). The cations initially adsorb to the membrane as a monolayer in a potential energy well at the level of the fatty acid carboxyl groups. The cations then pass through the hydrophobic core of the membrane to the potential energy well on the other side of the membrane before desorbing into the aqueous phase. This model suggests that the steady-state cation concentration in the membrane core is relatively low, and that their location is tightly constrained close to the membrane surfaces. However, it was not clear whether this model holds for TPP$^+$-conjugated to a very hydrophobic component, as is the case for MitoQ$_{10}$. Therefore, it remained uncertain whether MitoQ$_{10}$ was dissolved in the membrane core to a significant extent, or whether its TPP$^+$ component was constrained to a position near the membrane surface with the ubiquinone penetrating to a depth determined by the length of the alkyl linker. To address this issue, it was essential to understand better the position and orientation of MitoQ$_{10}$ bound to membranes. For this we studied the interaction of MitoQ$_{10}$ with phospholipid bilayers through collisional quenching of a series of fluorescent pyrene probes (14). The data obtained are consistent with a model in which the TPP$^+$ moiety is largely excluded from the hydrophobic core, while the ubiquinone is inserted into it. Thus the restricted orientation of MitoQ$_{10}$ is likely to explain the decreased reactivity of it with complex III. Our findings have significant implications for understanding of the interaction of MitoQ$_{10}$ and other mitochondria-targeted compounds with mitochondrial membranes and enzymes.

## EXPERIMENTAL PROCEDURES

*Materials*—CoQ$_1$, CoQ$_2$, decylQ, 1-pyrene acetic acid (Pyr$_2$), and 1-pyrene butanoic acid (Pyr$_4$) were from Sigma. 1-Pyrene hexanoic acid (Pyr$_6$) was from Fluka. 1-Pyrene decanoic acid (Pyr$_{10}$), 1-pyrene dodecanoic acid (Pyr$_{12}$), and 1-pyrene hexadecanoic acid (Pyr$_{16}$) were from Molecular Probes. MitoQ$_{10}$ and MitoQ$_{15}$ were synthesized as described previously (1, 2). TritylQ$_{10}$ was prepared from idebenol as outlined in on-line supplemental Fig. S1. Other ubiquinone analogs were sourced as described previously (15). The structures of some of these are shown in Fig. 1*A*.

*Fluorescence Quenching*—To prepare small unilamellar vesicles (SUV), 4.8 $\mu$l of 10 mM 1-pyrene carboxylic acid in Me$_2$SO and 480 $\mu$l of either 25 mg·ml$^{-1}$ turkey egg yolk L-$\alpha$-phosphatidyl choline (PC; ~60% PC, Type XII-E, Sigma) or 25 mg·ml$^{-1}$ soybean asolectin (~55% PC, Type IV-S, Sigma) in chloroform were evaporated to dryness under a stream of nitrogen in a 15-ml glass Kimax tube. Residual chloroform was removed under vacuum before 12 ml of KP$_i$ buffer (50 mM KP$_i$-KOH (pH 7.8), 100 $\mu$M EDTA, and 100 $\mu$M diethylenetriaminepentaacetic

acid) was added followed by incubation for 1 h at room temperature. The tube was then vortexed vigorously and placed in a Decon F5 Minor sonicating water bath for 30 min at room temperature. To assess the size distribution of the egg yolk SUV preparation, 2 $\mu$l was adsorbed to a Cu/Rh grid for 2 min before blotting. Uranyl acetate (1%) was immediately applied for 8 s before thorough blotting. The grids were visualized using a Tecnai 12 electron microscope at ×26,000 magnification. The SUVs had a mean external spherical diameter of 86 nm with a S.D. of 26 nm ($n = 35$).

Pyrene quenching was assayed in 2.5 ml of the SUV suspension (1 mg·ml$^{-1}$) in a stirred cuvette with a Shimadzu RF 5301-PC fluorimeter ($\lambda_{ex}$ 343–346 ± 1.5 nm, $\lambda_{em}$ 377 ± 0.75 nm) at 30 °C. Five 2-$\mu$l additions from 10 mM stock solutions of $MitoQ_{10}$, decylQ, idebenone, or decylTPP in ethanol were made at 30–60 s intervals, and the fluorescence measured before ($I_0$) and after (I) each addition. Fluorescence quenching was plotted as $I_0/I - 1$ *versus* the concentration (mM) of $MitoQ_{10}$, decylQ, idebenone, or decylTPP, with the slope of the line being the Stern-Volmer (SV) constant (14). The loss of $Pyr_2$ fluorescence upon ubiquinone addition in bulk phase ethanol was assumed to result from an inner filter effect, and the values for $I_0$ and I were corrected accordingly. Correction for the inner filter effect decreased the SV constants in SUVs and mitochondrial membranes when a ubiquinone was the quencher by ~1 mM$^{-1}$. Experiments with decylTPP showed there was no inner filter effect due to the $TPP^+$ moiety.

Bovine heart mitochondria were isolated, and mitochondrial membranes were prepared from these as described previously (16, 17). For fluorescence quenching of 1-pyrene carboxylic acids, bovine heart mitochondrial membranes (800 $\mu$g protein·ml$^{-1}$) were added to a stirred cuvette containing 2.5 ml of $KP_i$ buffer in a Shimadzu RF 5301-PC fluorimeter ($\lambda_{ex}$ 343–346 ± 1.5 nm, $\lambda_{em}$ 377 ± 0.75 nm) at 37 °C. To this was added 1 $\mu$l of 10 mM 1-pyrene carboxylic acid in $Me_2SO$ and once the fluorescence had stabilized, fluorescence quenching was determined as above. Binding of 1-pyrene carboxylic acids to bovine heart mitochondrial membranes (800 $\mu$g of protein) was measured by incubating them in 1 ml of $KP_i$ buffer containing 20 $\mu$M 1-pyrene carboxylic acid for 10 min at 37 °C. Membranes were pelleted by centrifugation (30 min at 16,000 × *g*, 37 °C), after which the supernatant was removed and extracted 1–3 times with 1 ml of octan-1-ol. The fraction of pyrene carboxylic acid in the aqueous phase was determined by measuring the $A_{345}$ of the combined octan-1-ol extracts and comparing it to the $A_{345}$ of the original 1-pyrene carboxylic acid solution in octan-1-ol. The concentration of $Pyr_{16}$ in the aqueous phase was too low to be measured accurately and thus all $Pyr_{16}$ was assumed to be membrane associated.

*Solvent Solubility*—Serial dilutions of a 100 mM ethanol stock of the relevant ubiquinone were evaporated to dryness under vacuum in a 1.5-ml Eppendorf tube. The ubiquinone (3–1000 nmol) was then resuspended in 1 ml of octan-1-ol or cyclohexane with vigorous vortexing. As $MitoQ_{10}$ was minimally soluble in cyclohexane and formed a separate orange phase, attempts were made to solubilize it further by placing it for 3 h in a shaking water bath at 37 °C or for 30 min in a Decon F5 Minor sonicating water bath. $MitoQ_{10}$ was solubilized to the same extent in cyclohexane after either treatment. After centrifugation (30 s at 13,000 × *g*) the $A_{275}$ of the supernatant was measured to calculate the ubiquinone concentration.

*Protein Purification*—Porcine ETF-QOR was purified from porcine liver submitochondrial particles as described previously (18). Human ETF and human medium chain acyl-CoA dehydrogenase (MCAD) were expressed from pET vectors in *Escherichia coli* and purified (19, 20). Complex I was purified from bovine heart mitochondria (21). Complex II was partially purified from bovine heart mitochondria. Briefly, mitochondria were solubilized in 20 mM Tris-HCl (pH 8), 1% (w/v) dodecylmaltoside, 500 $\mu$M EDTA. After centrifugation, the supernatant was applied to a Q-Sepharose column in 20 mM Tris-HCl, pH 8, 0.1% (w/v) dodecylmaltoside, 50 mM sucrose, 2 mM $MgSO_4$, 1 mM EDTA, 10% (v/v) glycerol. Protein was eluted using a linear gradient of 0–500 mM NaCl with complex II eluting at ~200 mM NaCl. Fractions containing complex II activity were pooled and concentrated using a 100-kDa cutoff spin column (Vivascience) then applied to a 1.6 × 60 cm S-300 column equilibrated with 20 mM Tris-HCl (pH 8), 0.1% (w/v) dodecylmaltoside, 50 mM sucrose, 2 mM $MgSO_4$, 1 mM EDTA, 10% (v/v) glycerol, 200 mM NaCl. Fractions containing complex II were pooled and concentrated using a 100-kDa cutoff spin column.

*Isolated Enzyme Assays*—ETF-QOR was assayed in a reaction mixture containing 10 mM Hepes-KOH (pH 7.4), 1 $\mu$M MCAD, 1 $\mu$M ETF, 100 $\mu$M octanoyl-CoA, 6 mM CHAPS, and 60 $\mu$M of either $CoQ_2$, decylQ, idebenone, tridecylQ, $MitoQ_{10}$, or $MitoQ_{15}$ at 25 °C. The reaction was initiated by the addition of ETF-QOR and monitored as the decrease in absorbance at 275 nm ($\epsilon_{ox\text{-}red}$ = 7.4 mM$^{-1}$·cm$^{-1}$; this extinction coefficient accounts for the contribution of octenoyl-CoA at 275 nm (18, 22)).

Ubiquinone reduction by isolated complex I was assayed in a stirred cuvette containing 20 mM Hepes-KOH (pH 7.5), 50 $\mu$M $NAD^+$, 500 $\mu$g·ml$^{-1}$ asolectin, 0.05% (w/v) CHAPS, 5 mM lactate, 5 units·ml$^{-1}$ lactate dehydrogenase, and 10 $\mu$M of either decylQ or $MitoQ_{10}$ at 32 °C. After a 2-min preincubation, the reaction was initiated by addition of ~2 $\mu$g·ml$^{-1}$ isolated complex I and monitored by measuring the decrease in $A_{275}$. Rotenone (8 $\mu$g·ml$^{-1}$) was added as indicated. Asolectin (Fluka) was partially purified by several rounds of precipitation with acetone (23), stored under nitrogen at −20 °C, and added as a 10 mg·ml$^{-1}$ stock in 1% (w/v) CHAPS, 20 mM Hepes-KOH (pH 7.5). NADH oxidation by isolated complex I was assayed in a reaction mixture containing 20 mM Hepes-KOH (pH 7.5), 100 $\mu$M NADH, 500 $\mu$g·ml$^{-1}$ asolectin, 0.05% (w/v) CHAPS, and 200 $\mu$M of either decylQ or $MitoQ_{10}$ at 32 °C. The reaction was initiated by addition of ~2 $\mu$g·ml$^{-1}$ isolated complex I and measured as a decrease in $A_{340-380}$. Some assays also contained 8 $\mu$g·ml$^{-1}$ rotenone.

Ubiquinone reduction by isolated complex II was assayed in a stirred cuvette containing 20 mM Hepes-KOH (pH 7.5), 5 mM succinate, 500 $\mu$g·ml$^{-1}$ asolectin, 0.05% (w/v) CHAPS, and 50 $\mu$M of either decylQ, idebenone, or $MitoQ_{10}$ at 32 °C. The reaction was initiated by addition of ~10 $\mu$g·ml$^{-1}$ isolated complex II and measured as a decrease in $A_{275}$ ($\epsilon_{ox\text{-}red}$ = 12.5 mM$^{-1}$·cm$^{-1}$).

*Enzyme Assays in Bovine Heart Mitochondrial Membranes*—Although tritylQ$_{10}$ is soluble in octan-1-ol and cyclohexane up to 1 mM (data not shown), it is significantly more hydrophobic than MitoQ$_{10}$. Direct addition to lipid containing buffer results in slow or uneven incorporation into bilayers as judged by fluorescence quenching of Pyr$_{12}$ (data not shown). As this effect was also observed with CoQ$_4$ it was used as a control. Incorporation of tritylQ$_{10}$ or CoQ$_4$ into phospholipids could be achieved by either sonication or reconstitution from chloroform. However, as conditions could not be easily achieved where either CoQ$_4$ or tritylQ$_{10}$ were substrates for isolated complex I or complex II, we used bovine heart mitochondrial membranes sonicated in the presence of tritylQ$_{10}$ or CoQ$_4$.

Ubiquinone reduction by NADH in bovine heart mitochondrial membranes (100 $\mu g \cdot ml^{-1}$) was assayed in 20 mM Hepes-KOH (pH 7.5), 50 $\mu$M NAD$^+$, 5 mM lactate, 200 $\mu$M KCN, and 50 $\mu$M of either CoQ$_4$, tritylQ$_{10}$, decylQ, or MitoQ$_{10}$ at 32 °C. After microtip sonication (Misonix 3000; 6 × 5 s, 0 °C) in a glass vial the reaction mix was transferred to a stirred cuvette. Following preincubation, the reaction was initiated by addition of lactate dehydrogenase (5 units·ml$^{-1}$) and monitored by measuring the decrease in $A_{275}$. No decrease in $A_{275}$ occurred in the absence of ubiquinone or presence of 8 $\mu g \cdot ml^{-1}$ rotenone.

Ubiquinone reduction by succinate in bovine heart mitochondrial membranes (100 $\mu g \cdot ml^{-1}$) was assayed in 20 mM Hepes-KOH (pH 7.5), 200 $\mu$M KCN, 8 $\mu g \cdot ml^{-1}$ rotenone, and 50 $\mu$M of either CoQ$_4$, tritylQ$_{10}$, decylQ, or MitoQ$_{10}$ at 32 °C. After microtip sonication (6 × 5 s, 0 °C) in a glass vial the reaction mix was transferred to a stirred cuvette. Following a 2-min preincubation, the reaction was initiated by addition of 5 mM succinate and monitored by measuring the decrease in $A_{275}$. No decrease in $A_{275}$ occurred in the presence of 20 mM malonate.

Ubiquinol oxidation by bovine heart mitochondrial membranes (50 $\mu g \cdot ml^{-1}$) was assayed in 20 mM Hepes-KOH (pH 7.5), 8 $\mu g \cdot ml^{-1}$ rotenone, 200 $\mu$M KCN, and 50 $\mu$M of the ubiquinol form of either CoQ$_4$, tritylQ$_{10}$, decylQ, or MitoQ$_{10}$ at 32 °C. After microtip sonication (6 × 5 s, 0 °C) in a glass vial the reaction mix was transferred to a stirred cuvette. Following a 2-min preincubation, the reaction was initiated by addition of 50 $\mu$M cytochrome *c* and monitored by measuring the increase in $A_{550}$ ($\epsilon_{red\text{-}ox}$ = 21 $mM^{-1} \cdot cm^{-1}$). The increase in $A_{550}$ in the presence of 400 nM myxothiazol was subtracted. Ubiquinone was reduced by NaBH$_4$, extracted and stored in ethanol (pH 2) as described previously (3).

## RESULTS

*MitoQ$_{10}$ Is a Good Substrate for Isolated Complex II but a Poor Substrate for Isolated ETF-QOR and Complex I*—In order for MitoQ$_{10}$ to function as a recyclable antioxidant, effective reduction to its ubiquinol form within mitochondria is essential. We had previously observed poor reduction of MitoQ$_{10}$ by complex I in bovine heart mitochondrial membranes (3). However, these membranes contain endogenous CoQ$_{10}$ and several enzyme active sites that could catalyze redox exchange between CoQ$_{10}$ and MitoQ$_{10}$. Furthermore, we did not know whether electrons from $\beta$-oxidation, via electron-transferring flavoprotein:quinone oxidoreductase (ETF-QOR) could reduce MitoQ$_{10}$. To investigate the interaction of MitoQ$_{10}$ with the major sites of ubiquinone reduction we isolated complex I, complex II, and ETF-QOR and assayed their ability to reduce MitoQ$_{10}$.

When isolated complex II (succinate dehydrogenase) was incubated with MitoQ$_{10}$ the rate of ubiquinone reduction was identical to that for idebenone and decylQ (Fig. 1*B*). This confirms that MitoQ$_{10}$ is a good substrate for this enzyme and is consistent with previous observations in bovine heart mitochondrial membranes (3). Complex I (NADH:ubiquinone oxidoreductase) is the route by which electrons enter the CoQ pool from mitochondrial NADH. When we incubated MitoQ$_{10}$ or MitoQ$_{15}$ with isolated complex I in the presence of supplementary phospholipids no rotenone-sensitive ubiquinol generation (supplemental Fig. S2) or NADH oxidation (Fig. 1*C*), was observed. These results contrast with those when decylQ was used as an electron acceptor (Fig. 1*C* and supplemental Fig. S2) and demonstrate that MitoQ$_{10}$ and MitoQ$_{15}$ are not substrates for isolated complex I, consistent with previous observations in mitochondrial membranes (3). During $\beta$-oxidation ETF-QOR accepts electrons from the soluble protein ETF, and in turn donates these to the CoQ pool. When isolated ETF-QOR was incubated with MitoQ$_{10}$ or MitoQ$_{15}$ the rates of reduction to the ubiquinol form were slow (Fig. 1*D*). As decylQ, idebenone and a range of other ubiquinone derivatives are readily reduced by ETF-QOR (Fig. 1*D*) (15), it is concluded that the TPP$^+$ moiety inhibits access of MitoQ$_{10}$ and MitoQ$_{15}$ to the ubiquinone reduction site in ETF-QOR.

In summary, MitoQ$_{10}$ is a good substrate for isolated complex II, but a poor substrate for isolated ETF-QOR and complex I. Therefore complex II appears primarily responsible for reducing MitoQ$_{10}$ *in vivo*. We note that while glycerol-3-phosphate dehydrogenase can reduce MitoQ$_{10}$ (3), its location on the outer surface of the mitochondrial inner membrane and low expression in many tissues may limit its importance *in vivo*.

*The Bulkiness of Its TPP$^+$ Moiety Contributes to the Poor Reactivity of MitoQ$_{10}$ with Complex I and ETF-QOR, but Not Complex III*—Having determined the likely site of MitoQ$_{10}$ reduction within mitochondria, our aim was to understand why MitoQ$_{10}$ was not reduced by ETF-QOR or complex I (Fig. 1), or oxidized by complex III (3). Three possible explanations exist for the poor reactivity of MitoQ$_{10}$ with ETF-QOR, complex I and complex III; either the ubiquinone binding site is in a hydrophobic environment to which the positive charge of the TPP$^+$ moiety prevents access, there is a long narrow access channel that the bulky TPP$^+$ moiety cannot enter or they are inhibited by MitoQ$_{10}$. Recently the structure of ETF-QOR was determined and shown to have a long narrow ubiquinone binding channel (24). Overlaying MitoQ$_{10}$ with the ubiquinone moiety and five isoprenoid units of CoQ$_{10}$ visible in the ETF-QOR structure clearly indicates that the TPP$^+$ moiety of MitoQ$_{10}$ prevents its ubiquinone group from reaching the ubiquinone binding site of ETF-QOR (data not shown). Thus, steric hindrance caused by the bulkiness of its TPP$^+$ moiety is sufficient to explain the lack of reactivity of MitoQ$_{10}$ with ETF-QOR. In contrast, molecular modeling of MitoQ$_{10}$ with complex III shows that the TPP$^+$ moiety does not sterically prevent access of the ubiquinone group to active sites within complex III (3), suggesting an alternative explanation (see below).

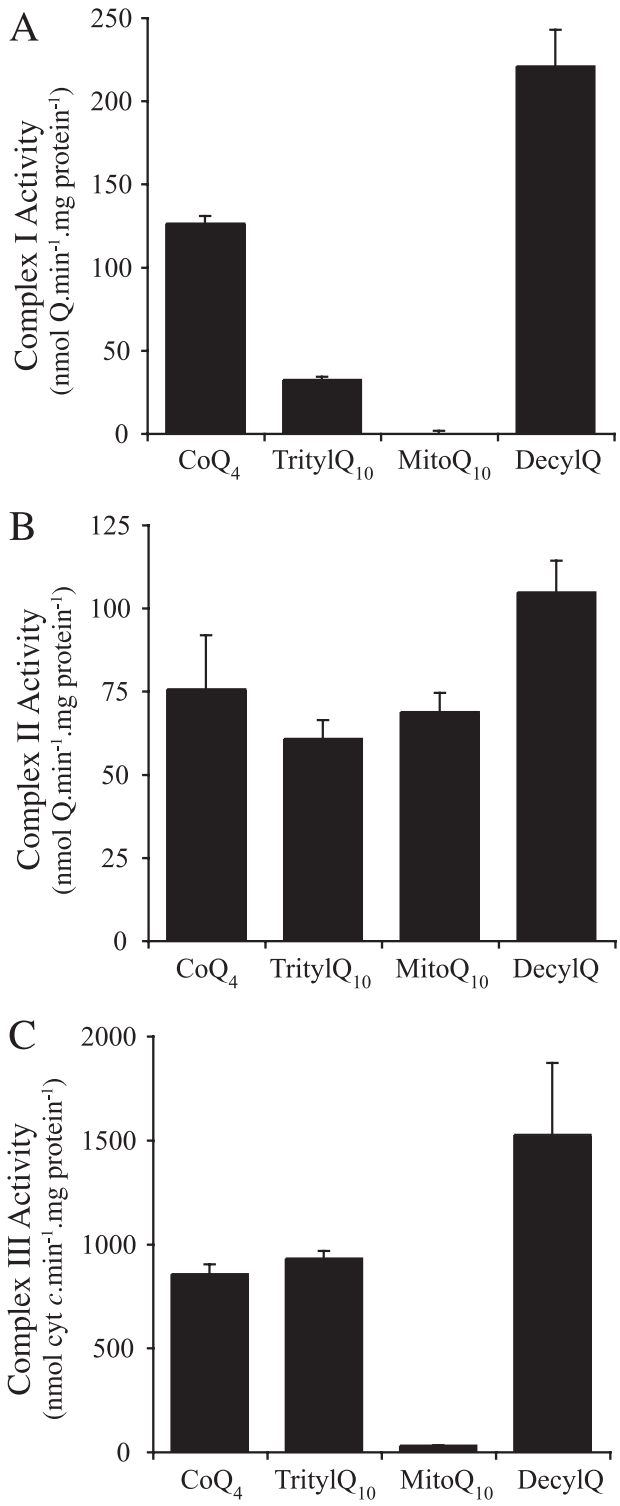


FIGURE 2. **TritylQ$_{10}$, an uncharged, but sterically similar MitoQ$_{10}$ analog, shows that steric hindrance contributes to the poor reactivity of MitoQ$_{10}$ with complex I.** *A*, MitoQ$_{10}$ and tritylQ$_{10}$ are both poorly reduced by complex I. Rotenone-sensitive ubiquinone reduction by NADH in bovine heart mitochondrial membranes (100 $\mu$g·ml$^{-1}$) was assayed in buffer containing NAD$^+$, lactate, and 50 $\mu$M of either CoQ$_4$, tritylQ$_{10}$, decylQ, or MitoQ$_{10}$. The reaction was initiated by addition of 5 units·ml$^{-1}$ lactate dehydrogenase and monitored by measuring the decrease in $A_{275}$. The decrease in $A_{275}$ in the absence of ubiquinone or presence of 8 $\mu$g·ml$^{-1}$ rotenone was minimal, but still subtracted. Data are the means ± S.E. of three experiments. *B*, both MitoQ$_{10}$ and tritylQ$_{10}$ are effectively reduced by complex II. Malonate-sensitive ubiquinone reduction by succinate in bovine heart mitochondrial membranes (100 $\mu$g·ml$^{-1}$) was assayed in buffer with 50 $\mu$M of either CoQ$_4$, tritylQ$_{10}$, decylQ, or MitoQ$_{10}$. The reaction was initiated by addition of 5 mM succinate and monitored by measuring the decrease in $A_{275}$. The rate in the presence of 20 mM malonate was negligible, but still subtracted. Data are the means ± S.E. of three experiments. *C*, tritylQ$_{10}$, but not MitoQ$_{10}$, is oxidized by complex III. Myxothiazol-sensitive ubiquinol oxidation by bovine heart mitochondrial membranes (50 $\mu$g·ml$^{-1}$) was assayed in buffer containing 50 $\mu$M of the ubiquinol form of either CoQ$_4$, tritylQ$_{10}$, decylQ, or MitoQ$_{10}$. The reaction was initiated by addition of 50 $\mu$M cytochrome *c* and monitored by measuring the increase in $A_{550}$. The increase in $A_{550}$ in the presence of 400 nM myxothiazol was significant and subtracted. Data are the means ± S.E. of three experiments.

Unlike ETF-QOR and complex III, there is little structural information available about the ubiquinone binding site(s) of complex I (25). To differentiate between the first two possibilities we synthesized a similar sized but uncharged analog of MitoQ$_{10}$ in which the positively charged phosphonium at the center of the TPP$^+$ moiety is replaced by a neutral carbon (tritylQ$_{10}$; Fig. 1*A*). In contrast to MitoQ$_{10}$, tritylQ$_{10}$ is very lipophilic and will easily permeate into the hydrophobic core of the membrane. Therefore if tritylQ$_{10}$ is not a substrate for complex I, it would imply that the large size of its terminal TPP$^+$ moiety contributes to the lack of MitoQ$_{10}$ reduction by complex I. Reduction and oxidation of tritylQ$_{10}$ was compared with CoQ$_4$ as both required sonication for effective incorporation into membranes (see "Experimental Procedures"). TritylQ$_{10}$ is a less effective substrate for complex I than CoQ$_4$ (Fig. 2*A*), suggesting that the steric effect is important in this case. This appears to be compounded by the charge of the TPP$^+$ moiety as MitoQ$_{10}$ is even less reactive than tritylQ$_{10}$ (Fig. 2*A*). In contrast to complex I, both tritylQ$_{10}$ and CoQ$_4$ are good substrates for complexes II and III (Fig. 2, *B* and *C*) consistent with the lack of steric hindrance previously indicated by molecular modeling of MitoQ$_{10}$ with these complexes (3). However, contrary to tritylQ$_{10}$, the reduced form of MitoQ$_{10}$ is poorly oxidized by complex III, suggesting that steric hindrance does not prevent access of MitoQ$_{10}$ to the active sites of complex III. Instead it is the charge on MitoQ$_{10}$ that limits its reactivity, possibly by preventing a high concentration of MitoQ$_{10}$ in the membrane. In summary, steric hindrance does not play a role in the low reactivity of MitoQ$_{10}$ with complex III, but certainly contributes to the slow reduction of MitoQ$_{10}$ by complex I and ETF-QOR.

*Inhibition of Complexes I and III Is Not Responsible for Their Poor Reactivity with MitoQ$_{10}$*—One potential explanation for the poor reactivity of MitoQ$_{10}$ with complexes I and III is that high concentrations of lipophilic cations can inhibit mitochondrial function. Consistent with this in bovine heart mitochondrial membranes there is some evidence of inactivation of complexes I and III in the presence of 50 $\mu$M decylTPP (data not shown). To confirm that the lack of MitoQ$_{10}$ reactivity with complex I and III (Fig. 2) does not solely arise from inhibition or inactivation, we measured the rate of decylQ reactivity with these complexes in the presence of lower concentrations of both redox forms of MitoQ$_{10}$ or decylTPP. The rate of decylQ reduction by Complex I was not inhibited by either the reduced or the oxidized forms of MitoQ$_{10}$, or by decylTPP (supplemental Fig. S3*A*). In contrast, MitoQ$_{10}$ is largely unreactive with complex I when compared with decylQ in the presence of an equivalent amount of lipophilic cation (supplemental Fig. S3*A*). Similarly the rate of decylQ oxidation by complex III

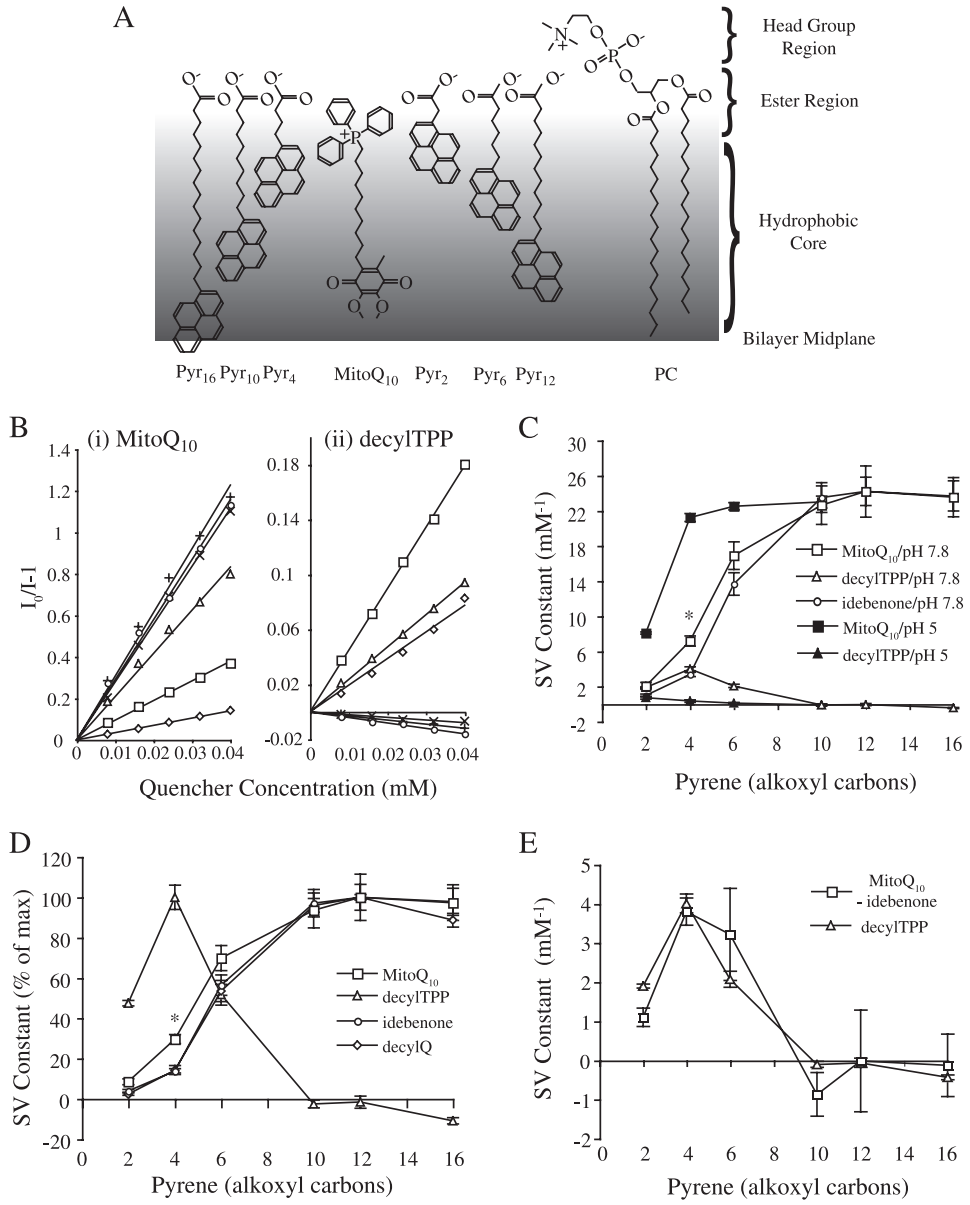


FIGURE 3. **Pyrene carboxylic acid quenching by $MitoQ_{10}$.** *A*, a model of the hydrophobic core of one leaflet of a phospholipid bilayer formed from phosphatidylcholine (*PC*) with a range of fluorescent 1-pyrene carboxylic acids ($Pyr_n$) and a collisional quencher, $MitoQ_{10}$. The dielectric constant of the hydrophobic core increases with distance from the bilayer midplane. *B*, examples of determining the Stern-Volmer (*SV*) constant for $MitoQ_{10}$ (i) and decylTPP (ii). Fluorescence was measured before ($I_0$) and after (I) serial additions of 8 $\mu$M quencher, in this case $MitoQ_{10}$ or decylTPP, were made to egg yolk small unilamellar vesicles (1 mg·ml$^{-1}$) containing 4 $\mu$M of either $Pyr_2$ (◇), $Pyr_4$ (□), $Pyr_6$ (△), $Pyr_{10}$ (×), $Pyr_{12}$ (+), or $Pyr_{16}$ (○). SV constants are the slope of $I_0/I - 1$ plotted against the $MitoQ_{10}$ or decylTPP concentration. *C*, fluorescence quenching of 1-pyrene carboxylic acids by decylTPP (△), idebenone (○), and $MitoQ_{10}$ (□) at pH 7.8 and decylTPP (▲) and $MitoQ_{10}$ (■) at pH 5.0 as a function of 1-pyrene carboxylic acid chain length. *D*, alkyl length at which decylTPP (△), idebenone (○), $MitoQ_{10}$ (□), and decylQ (◇) maximally quench 1-pyrene carboxylic acids at pH 7.8. *E*, the difference between $MitoQ_{10}$ and idebenone quenching (□) at pH 7.8 mimics quenching by decylTPP (△). All data are mean ± S.E. of three independent experiments. The statistical significance of pyrene quenching by $MitoQ_{10}$ relative to idebenone was determined using a Student's two-tailed *t* test: *, $p < 0.01$.

was not inhibited by the presence of either the reduced or the oxidized forms of $MitoQ_{10}$, or by decylTPP (supplemental Fig. S3*B*). Like complex I, $MitoQ_{10}$ is largely unreactive with complex III when compared with decylQ in the presence of an equivalent amount of lipophilic cation (supplemental Fig. S3*B*). While in both cases, there is some redox exchange between the two hydrophilic ubiquinones, decylQ and $MitoQ_{10}$, it is clear that complexes I and III are still active in the presence of both redox forms of $MitoQ_{10}$.

In summary, enzyme inhibition or inactivation does not explain the poor reactivity of $MitoQ_{10}$ with complexes I and III. That decylQ is oxidized in the presence of decylTPP, but $MitoQ_{10}$ is not, again clearly shows that it is the linking of a $TPP^+$ moiety to the ubiquinone group that inhibits $MitoQ_{10}$ reacting with complex III.

*The $TPP^+$ Moiety of $MitoQ_{10}$ Is Largely Excluded from the Hydrophobic Core of Phospholipid Bilayers While the Ubiquinone Moiety Is Not*—Although lipophilic cations such as $MitoQ_{10}$ are membrane permeable, their charged nature could mean that their steady-state concentration deep within phospholipid bilayers is minimal. This could explain the inability of $MitoQ_{10}$ to interact effectively with complex III. To determine whether the local distribution of the $TPP^+$ and ubiquinone moieties of $MitoQ_{10}$ in different regions of the phospholipid bilayer varies and hence to gauge its overall molecular orientation, we measured its ability to quench the fluorescence of a pyrene moiety separated from a carboxylic acid by a carbon chain of *n*-1 methylene groups ($Pyr_n$, $n = 2, 4, 6, 10, 12, 16$). This probe was chosen because at neutral pH the depth of the fluorescent pyrene label within the membrane will depend on the length of the chain between it and the carboxylate (14, 26). As a result, the chain length-dependence of pyrene fluorescence quenching gives an indication of the relative position of the quencher within a membrane, as illustrated in Fig. 3*A*. To determine the position of a quenching moiety within a membrane, we prepared small unilamellar vesicles (SUVs) from egg yolk phospholipids containing a range of these 1-pyrene carboxylic acids. We then measured fluorescence quenching of the incorporated pyrene moiety upon addition of increasing amounts of various quenching molecules, the structures of which are shown in Fig. 1*A*. The fluorescence before ($I_0$) and after (I) each addition of quencher was plotted *versus* the quencher concentration, the slope being the Stern-Volmer (SV)

constant. That the plot of $I_0/I - 1$ *versus* quencher concentration is linear indicates that quenching of pyrene fluorescence by $TPP^+$ and ubiquinone in SUVs is collisional (Fig. 3*B*) (14). $MitoQ_{10}$ strongly quenched $Pyr_{10-16}$ which will lie deep in the hydrophobic core of the membrane, but only weakly quenched $Pyr_2$ and $Pyr_4$, which will lie closer to the bilayer surface (Fig. 3, *C* and *D*). As $MitoQ_{10}$ is a composite of a ubiquinone group and a $TPP^+$ moiety (Fig. 1*A*), both of which might quench pyrenes, we next compared the fluorescence quenching of $MitoQ_{10}$ with decylTPP and idebenone (Fig. 3*C*). These compounds were chosen as they are structurally related to $MitoQ_{10}$, but lack the ubiquinone or $TPP^+$ moieties, respectively. To minimize discrepancies due to differences in quencher concentration in the lipid phase and/or quenching efficiency, and to facilitate comparison of the depth within the membrane of each quenching moiety, these data were replotted as a percentage of the SV constant of the pyrene carboxylic acid that quenched most strongly (Fig. 3*D*). Like $MitoQ_{10}$, the ubiquinone moiety of idebenone maximally quenches the deeper lying $Pyr_{10-16}$ with significantly less quenching of the shallower $Pyr_{2-6}$ (Fig. 3, *C* and *D*). In contrast, decylTPP exhibits maximal quenching with $Pyr_4$ and none at all with $Pyr_{10}$-$Pyr_{16}$ (Fig. 3, *C* and *D*), suggesting that the $TPP^+$ moiety is concentrated nearer the surface and does not have access to the core of the phospholipid bilayer. While the quenching profiles of $MitoQ_{10}$ and idebenone are similar, close inspection indicates that there are subtle differences. $Pyr_4$ is quenched significantly more by $MitoQ_{10}$ than idebenone ($p = 0.004$) and a relative increase in quenching by $MitoQ_{10}$ over idebenone is also observed with $Pyr_2$ and $Pyr_6$. In fact the difference between the quenching profiles of idebenone and $MitoQ_{10}$ is very similar to the profile for decylTPP (Fig. 3*E*) suggesting that quenching by the two moieties is additive. This implies that the $TPP^+$ moiety of $MitoQ_{10}$, like that of decylTPP, is found nearer the phospholipid bilayer surface while the ubiquinone group is buried within the bilayer.

The position of the carboxyl carbon of pyrene carboxylic acids is expected to be similar to that of anthroloxy-labeled fatty acids where the ionized carboxyl carbon resides 18.6 Å from the bilayer midplane, with the protonated uncharged form lying slightly deeper at 16 Å (26). This places the carboxyl carbon close to the depth of the ester carbonyl groups on the acyl chains of phospholipids (27). At pH 7.8, pyrene carboxylic acids are largely ionized while at pH 5 they will be ~50% neutral and thus will on average lie deeper within the membrane. In contrast, the net charges on the $TPP^+$ and ubiquinone moieties are pH-independent. Therefore lowering the pH to 5.0 should result in the pyrene moiety moving deeper into the membrane relative to the quenching groups. Consistent with this scenario, $MitoQ_{10}$ and idebenone were much more effective at quenching $Pyr_{2-6}$ at pH 5.0 than at pH 7.8 while decylTPP was largely ineffective at quenching any of the pyrenes at pH 5.0 (Fig. 3*C*). Thus this experimental system gives an indication of the position of the $TPP^+$ and ubiquinone moieties within the phospholipid bilayer.

DecylTPP, idebenone, and $MitoQ_{10}$ were used because they have similar hydrophobicities ($\log(P) = 3.7, 4.2, 3.4$, respectively in octan-1-ol:PBS) (3) and thus, all should partition predominantly (>90%) into SUVs under our conditions, assuming a phospholipid volume of ~1 $\mu l \cdot mg^{-1}$ (28). This is an important consideration as the observed quenching is a function of the concentrations of quencher and fluorophor actually in the lipid phase, and is thus dependent on their hydrophobicities. To demonstrate that the quenchers were predominantly in the lipid phase decylQ, a ubiquinone analog ~10-fold more hydrophobic than idebenone ($\log P = 5.5$ in octan-1-ol:PBS) (3), was used and showed a similar quenching profile to both idebenone and $MitoQ_{10}$ (Fig. 3*D*). Thus all the quenchers used were predominantly in the lipid phase, and the results are not compromised by small differences in quencher hydrophobicity. However, differential quencher partitioning became problematic for MitoQ derivatives with shorter chain lengths. When we compared $MitoQ_3$ ($\log P = 0.5$ in octan-1-ol:PBS) with propylTPP and a 3-carbon analog of the 10-carbon linked idebenone, the level of quenching was weak, indicating that most of the quencher was present in the aqueous phase, and that the results were susceptible to small differences in quencher hydrophobicity (data not shown). This caveat is also true for the shorter pyrene carboxylic acids, a proportion of which may not be in the lipid phase.

To evaluate and address this latter issue we changed to a mitochondrial membrane system where we could separate the lipid and aqueous phases and thus correct for the proportion of pyrene carboxylic acid in the aqueous phase. Additionally, while the above work demonstrates that the $TPP^+$ moiety of $MitoQ_{10}$ is excluded from the hydrophobic core of a phospholipid bilayer, this may not be physiologically relevant as mitochondrial membranes contain a high proportion of protein and have a different lipid composition. To test whether these factors would facilitate penetration of the $TPP^+$ moiety of $MitoQ_{10}$ into the hydrophobic core, and to correct for the proportion of pyrene carboxylic acid in the aqueous phase, we measured fluorescence quenching in membranes isolated from bovine heart mitochondria. When compared with egg yolk SUVs, experiments with decylTPP gave stronger fluorescence quenching of $Pyr_{6-12}$ in mitochondrial membranes (Fig. 4*A*). While this suggests the $TPP^+$ moiety of decylTPP can assume a slightly deeper position within mitochondrial membranes, it was ineffective at quenching $Pyr_{16}$, the deepest penetrating pyrene carboxylic acid. As heart mitochondrial membranes differ from egg yolk phospholipids in several potentially important ways, *e.g.* they contain large amounts of protein, a higher proportion of unsaturated fatty acids, cardiolipin and little cholesterol (29), it is difficult to assign a single reason for this increased penetration. However, to partially address this issue we tested the penetration of decylTPP$^+$ into soybean asolectin, which also has a high degree of unsaturation, but is free of cholesterol and has a significant proportion of negatively charged phospholipids. In asolectin there was a similar increase in quenching of $Pyr_{10-16}$ by decylTPP (Fig. 4*A*), suggesting the increased penetration of decylTPP into mitochondrial membranes may result from different lipid composition. In contrast to decylTPP, fluorescence quenching in mitochondrial membranes by $MitoQ_{10}$ was largely unaffected by differences between egg yolk SUVs and mitochondrial membranes (Fig. 4*A*).

To determine the proportion of each pyrene carboxylic acid that was membrane-associated, we measured the fraction of

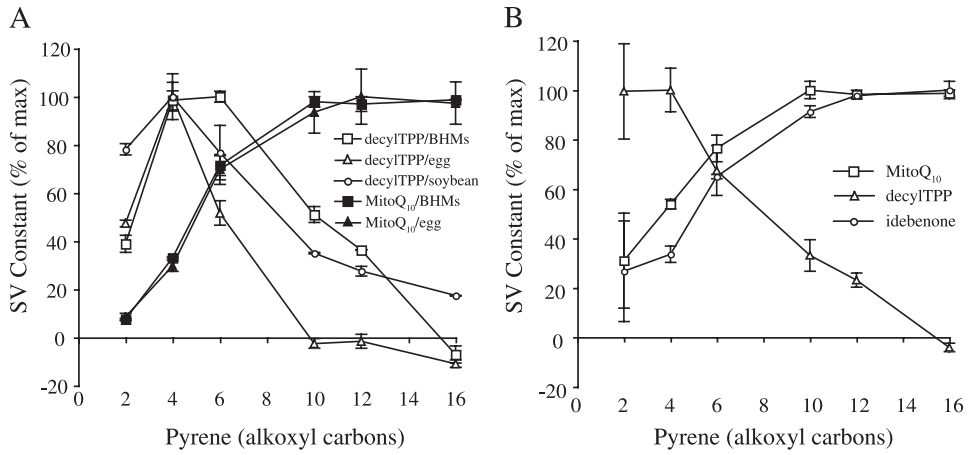


FIGURE 4. **The charged $TPP^+$ moiety of $MitoQ_{10}$ cannot quench pyrene fluorescence deep within the hydrophobic core of mitochondrial membranes.** *A*, the $TPP^+$ moiety of decylTPP quenches deeper 1-pyrene carboxylic acids in bovine heart mitochondrial membranes (BHMs) and soybean asolectin than in egg yolk phospholipids. Alkyl length at which decylTPP (△,○, and □) and $MitoQ_{10}$ (▲ and ■) maximally quench 1-pyrene carboxylic acids in egg yolk (△ and ▲), soybean asolectin (○) and BHMs (□ and ■). *B*, corrected alkyl length at which $MitoQ_{10}$ (□), decylTPP (△), and idebenone (○) maximally quench 1-pyrene carboxylic acid in BHMs. The data in *panel A* were corrected for the percentage of 1-pyrene carboxylic acid in the membrane phase and thus available for quenching. The percentage values used for $Pyr_2$, $Pyr_4$, $Pyr_6$, $Pyr_{10}$, $Pyr_{12}$, and $Pyr_{16}$ in the membrane phase were 24 ± 5, 61 ± 1, 93 ± 1, 97, 98, and 100, respectively. Data from egg yolk are means ± S.E. of three independent experiments. Data from BHMs and soybean asolectin are means ± range of two independent experiments.

each pyrene carboxylic acid in the aqueous phase. The percentages of $Pyr_2$, $Pyr_4$, $Pyr_6$, $Pyr_{10}$, and $Pyr_{12}$ in the aqueous phase were 76 ± 5, 39 ± 1, 7 ± 1, 3, and 2, respectively, while the percentage of $Pyr_{16}$ in the aqueous phase was negligible. When the data in Fig. 4*A* are corrected for the concentration of membrane-associated pyrene carboxylic acid, the true position of the $TPP^+$ moiety of decylTPP is evaluated as being closer to the membrane surface as indicated by enhanced quenching of $Pyr_2$ and $Pyr_4$ and the decreased relative quenching of $Pyr_{6-12}$ (Fig. 4*B*). Correction for pyrene carboxylic acid binding to mitochondrial membranes confirms that the ubiquinone moieties of both $MitoQ_{10}$ and idebenone are inserted into the membrane as they maximally quench $Pyr_{10-16}$. However, correction enhances the relative quenching of $Pyr_2$ and $Pyr_4$ (Fig. 4*B*), indicating the steady-state concentration of their ubiquinone moieties close to the membrane surface is higher in reality.

In summary, penetration of the ubiquinone moiety of $MitoQ_{10}$ into the membrane core is similar to uncharged ubiquinones such as idebenone and decylQ. In contrast, the $TPP^+$ moiety of $MitoQ_{10}$ is largely excluded from the hydrophobic core of phospholipid bilayers. Thus $MitoQ_{10}$ is orientated with its $TPP^+$ moiety near the surface of the membrane and its ubiquinone moiety inserted into the hydrophobic core of the lipid bilayer.

*The $TPP^+$ Moiety of $MitoQ_{10}$ Greatly Limits Its Solubility in Cyclohexane*—The quenching data indicate that the $TPP^+$ moiety of $MitoQ_{10}$ is predominantly localized to near the membrane surface while the ubiquinone moiety is present in the membrane core. That the ubiquinone moiety of $MitoQ_{10}$ can quench buried pyrenes as effectively as lipid soluble ubiquinones such as idebenone indicates that the concentration of the ubiquinone moiety of $MitoQ_{10}$ within the membrane core is high. However, a notable difference between idebenone and $MitoQ_{10}$ is that the $TPP^+$ moiety constrains the orientation of $MitoQ_{10}$ and the free movement of its attached ubiquinone moiety within the hydrophobic core. While this should not affect interactions between the ubiquinone moiety of $MitoQ_{10}$ and diffusible pyrenes or lipid radicals, access to a deeply buried ubiquinone binding site of a ubiquinone oxidoreductase might not be possible unless the $TPP^+$ moiety moves into the hydrophobic core of the membrane. In this case the concentration of the entire $MitoQ_{10}$ molecule in the hydrophobic core of the phospholipid lipid bilayer will become the important variable and for efficient reduction it would need to be of the order of the $K_m$ for $CoQ_{10}$ of mitochondrial ubiquinone oxidoreductases. To estimate the steady-state concentration of $MitoQ_{10}$ in the hydrophobic core of the membrane, we measured the solubility of $MitoQ_{10}$ in cyclohexane (relative dielectric constant ($\epsilon_r$) = 2) a solvent mimicking the hydrocarbon tail region of phospholipids in bilayers (30). $MitoQ_{10}$ was largely insoluble in cyclohexane with a maximum concentration of ~1–2 μM in solution (Fig. 5). In contrast, $MitoQ_{10}$ was very soluble in octan-1-ol ($\epsilon_r$ = 10.3), a more polar solvent that can form hydrogen bonds and mimics the ester region below the phospholipid head groups in membranes (Fig. 5). The insolubility of $MitoQ_{10}$ in cyclohexane was caused by the $TPP^+$ moiety as idebenone, a ubiquinone of similar structure that lacks the $TPP^+$ moiety, was freely soluble in both cyclohexane and octan-1-ol up to at least 1 mM (Fig. 5).

The relative insolubility of $MitoQ_{10}$ in cyclohexane could simply reflect insolubility induced by the counter-ion, methanesulfonate ($CH_3SO_3^-$), in cyclohexane. *In vivo* the dominant anion would be $Cl^-$ so to mimic this environment we incubated 300 nmol of $MitoQ_{10}$ with 1 ml of cyclohexane:100 μl of phosphate-buffered saline; however there was no increase in the solubility of $MitoQ_{10}$ in cyclohexane (data not shown). More hydrophobic anions may be available *in vivo* for ion pair formation thereby facilitating the solubilization of $MitoQ_{10}$ in the membrane. However, it was found that an equimolar amount (300 nmol) of sodium tetraphenylborate ($TPB^-$), a lipophilic anion that facilitates the membrane permeability of lipophilic cations (31, 32), failed to solubilize $MitoQ_{10}$ in cyclohexane (data not shown). As a result, we conclude that irrespective of the counter-ions available to it *in vivo*, $MitoQ_{10}$ will have low solubility in the non-polar hydrocarbon environment of the membrane core.

In summary, although $MitoQ_{10}$ is very soluble in octan-1-ol and will thus easily access the periphery of the bilayer, the solubility of $MitoQ_{10}$ in cyclohexane is ~2 μM. This indicates that the steady-state concentration of the entire $MitoQ_{10}$ molecule within the hydrophobic core of the phospholipid bilayer is likely to be significantly lower than the membrane concentra-

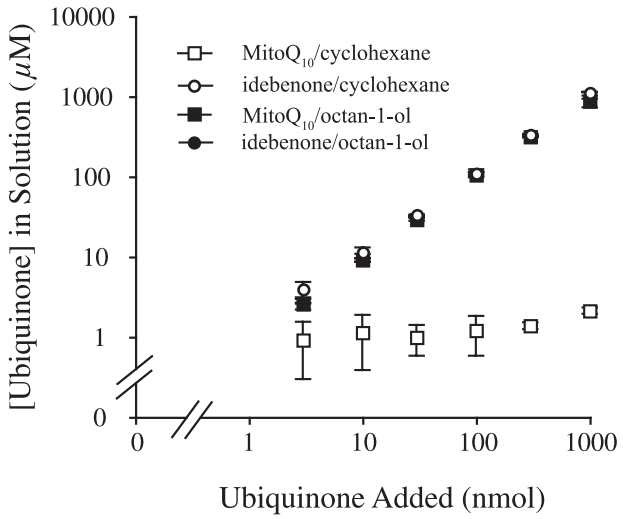


FIGURE 5. **$MitoQ_{10}$ is largely insoluble in cyclohexane, a solvent mimicking the hydrophobic core of phospholipid bilayers.** Varying amounts of either $MitoQ_{10}$ (□ and ■) or idebenone (○ and ●) were resuspended in 1 ml of either cyclohexane (□ and ○) or octan-1-ol (■ and ●), and the concentration in solution calculated by measuring $A_{275}$. Data are means ± range of two independent experiments.

tion of endogenous CoQ (1–10 mM) in mitochondria from a range of tissues and species (33, 34). As estimates of the $K_m$ for $CoQ_{10}$ of various mitochondrial ubiquinone oxidoreductases are of that order (34–36), we conclude that the poor reactivity of $MitoQ_{10}$ with mitochondrial complex III could easily result from the low steady-state concentration of $MitoQ_{10}$ in non-polar environments, such as the membrane core.

## DISCUSSION

Here we have shown that the $TPP^+$ moiety of $MitoQ_{10}$ resides largely on the membrane surface with its ubiquinone group buried within the hydrophobic core of the bilayer. This conclusion is based on the observations that decylQ and idebenone, but not decylTPP, can quench 1-pyrene carboxylic acids where the pyrene is deep within the membrane core (Figs. 3 and 4), and that $MitoQ_{10}$ has a low solubility in cyclohexane, a solvent mimicking the hydrophobic core (Fig. 5). Thus, although $TPP^+$-conjugated compounds can pass readily through phospholipid bilayers, the steady-state concentration of the $TPP^+$ moiety within the membrane core is very low. Instead, the $TPP^+$ moiety is located near the membrane surface with the extent of penetration of the attached group into the membrane determined by the length of the chain linking them. This orientation of $MitoQ_{10}$ leads to similar concentrations of the ubiquinone moiety within the membrane as occurs with short chain ubiquinone analogs such as idebenone or decylQ (Fig. 3*C*). This is significant for the antioxidant action of $MitoQ_{10}$ as it suggests that its active ubiquinol moiety would have free access to lipid radicals throughout the membrane core.

Even though incubation with $MitoQ_{10}$ led to similar concentrations of the ubiquinone moiety within the membrane as were found on incubation with short-chain ubiquinone analogs (Figs. 3 and 4), their interactions with ubiquinone oxidoreductases were dramatically different (Figs. 1 and 2). The concentration of the ubiquinone moiety, not the whole $MitoQ_{10}$ molecule, in the membrane will be the important determinant in the quenching reaction with 1-pyrene carboxylic acids as there is no requirement for the $TPP^+$ moiety to move into the hydrophobic core for an interaction between pyrene and ubiquinone to take place. In contrast, the ubiquinone binding sites of ubiquinone oxidoreductases are of a fixed depth and access from the direction of the membrane surface may be sterically hindered. If the $TPP^+$ moiety of $MitoQ_{10}$ had to move into a hydrophobic environment for its ubiquinone moiety to reach the active site, this would be thermodynamically unfavorable; in this case the concentration of the entire $MitoQ_{10}$ molecule, not its ubiquinone moiety, in the membrane core would become the relevant variable. As shown in Fig. 5 the concentration of the entire $MitoQ_{10}$ molecule in the membrane core is much lower than uncharged ubiquinones.

Reduction of $MitoQ_{10}$ to a ubiquinol by mitochondrial ubiquinone reductases is essential for its antioxidant function *in vivo*. Additionally, subsequent oxidation of $MitoQ_{10}$ by complex III would be required for it to function as an effective electron carrier in oxidative phosphorylation. Here we show that the interaction of $MitoQ_{10}$ with mitochondrial ubiquinone oxidoreductases is significantly different from that of artificial short-chain ubiquinone analogs, such as decylQ or idebenone. These findings indicate that $MitoQ_{10}$ is not effectively reduced to its antioxidant form by complex I or ETF-QOR, and that the principal mitochondrial enzyme responsible for reducing $MitoQ_{10}$ to its ubiquinol form *in vivo* is complex II. This is supported by further measurements in heart mitochondrial membranes where the physiological ratios of respiratory complexes are conserved; the absolute rate of $MitoQ_{10}$ reduction was 138 nmol·min$^{-1}$·mg protein$^{-1}$ for succinate compared with 4 nmol·min$^{-1}$·mg protein$^{-1}$ for NADH and 3.7 nmol·min$^{-1}$·mg protein$^{-1}$ for glycerol-3-phosphate (3). This level of $MitoQ_{10}$ reduction by complex II is clearly sufficient for it to function as a highly effective antioxidant in preventing mitochondrial oxidative damage *in vivo* (1–3,5). In contrast, $MitoQ_{10}$ is poorly oxidized by complex III suggesting it would be an ineffective replacement for $CoQ_{10}$ in oxidative phosphorylation.

Can the reactivity of $MitoQ_{10}$ be rationalized with what is known about the structures of the various mitochondrial ubiquinone oxidoreductases? Complex II is a transmembrane protein with a ubiquinone binding site near the matrix surface of the membrane (37). The ubiquinone binding site of complex II is accessed via a short channel which the ubiquinone moiety of $MitoQ_{10}$ can access while the $TPP^+$ moiety remains on the membrane surface (3). Consistent with this, the rate of reduction of $MitoQ_{10}$ and short-chain ubiquinones by complex II was identical (Figs. 1 and 4), indicating that all compounds could easily access its ubiquinone binding site. While the access channel is too short to sterically hinder $MitoQ_{10}$, molecular modeling indicates steric hindrance of $MitoQ_3$, and $MitoQ_3$ is a less effective substrate for complex II (3).

In contrast, $MitoQ_{10}$ is not oxidized by complex III (Fig. 2) and is not reduced by ETF-QOR or complex I, even though the other short-chain ubiquinone analogs were (Figs. 1 and 2). This occurs despite similar concentrations of the ubiquinone moieties of $MitoQ_{10}$, idebenone and decylQ within the membrane (Fig. 3*C*). One possible explanation for the lack of reactivity is

that the ubiquinone binding sites of complex I, complex III and ETF-QOR have long, narrow access channels to which entry of $MitoQ_{10}$ is sterically hindered by its $TPP^+$ moiety. A second potential reason is that the ubiquinone binding site is not sterically hindered, but is buried within the hydrophobic core of the membrane where the concentration of $MitoQ_{10}$ is low. A further consideration for the latter explanation is that the long hydrophobic tail of $CoQ_{10}$ resides in the midplane of phospholipid bilayers (34). Such a location for $CoQ_{10}$ requires that ubiquinone oxidoreductases have ubiquinone-binding sites that can be entered from the core of the membrane, often at the expense of access from the direction of the membrane surface. Entry of the ubiquinone moiety of $MitoQ_{10}$ to ubiquinone binding sites facing the midplane could thus be hindered as it would be thermodynamically unfavourable for $MitoQ_{10}$ to take on the required orientation, *i.e.* with its $TPP^+$ moiety in the hydrophobic core of the membrane.

ETF-QOR is a monotopic membrane protein with the molecular structure depicting five isoprenoids from $CoQ_{10}$ entering the ubiquinone reduction site from the lipid phase via a channel at the base of the enzyme (24). When $MitoQ_{10}$ is modeled into this active site the bulky $TPP^+$ moiety sterically hinders access of the ubiquinone group and this would appear sufficient to prevent $MitoQ_{10}$ reacting with ETF-QOR (data not shown). However, as $CoQ_{10}$ enters from the direction of the bilayer midplane and the $TPP^+$ of $MitoQ_{10}$ would need to enter the lipid phase for its ubiquinone to reach the active site, both mechanisms could in principle contribute to the lack of reactivity of $MitoQ_{10}$ with ETF-QOR. There is no molecular structure for the ubiquinone binding site(s) of complex I (25). Here we showed that while $tritylQ_{10}$ can be reduced by complex I, this rate is slower than $CoQ_4$, but faster than $MitoQ_{10}$ (Fig. 2*A*). This indicates that steric hindrance is a substantial component of the diminished reactivity of $MitoQ_{10}$ with complex I. This may be amplified by the low concentration of $MitoQ_{10}$ in the membrane core. Complex III contains both a ubiquinone reduction site and a ubiquinol oxidation site, each of which is nearer to and accessed from the direction of the bilayer midplane. The structure of complex III indicates that $MitoQ_{10}$ can enter both ubiquinone binding sites of complex III without steric hindrance (3, 38). Here we confirm this by showing that a neutral, sterically similar version of $MitoQ_{10}$, $tritylQ_{10}$, can be oxidized by complex III (Fig. 2*C*). As steric hindrance is not a factor and the ubiquinone binding sites of complex III are buried within the hydrophobic core, we conclude that $MitoQ_{10}$ is weakly oxidized by complex III primarily because the positive charge of the $TPP^+$ tethers the ubiquinone group to the membrane surface.

That the effective interaction of $MitoQ_{10}$ with enzyme active sites could be limited by tethering of its ubiquinone group to a $TPP^+$ moiety constrained to near the membrane surface, is further supported by the low $\mu$M steady-state concentration of the entire $MitoQ_{10}$ molecule in a solvent mimicking the bilayer core (Fig. 5). This concentration is far lower than that of $CoQ_{10}$ in mitochondrial membranes (~5 mM) (33, 34). Furthermore, estimates of the $K_m$ for endogenous $CoQ_{10}$ for NADH, succinate and glycerol-3-phosphate oxidation in the lipid phase are 5 mM, 500 $\mu$M, and 700 $\mu$M (34–36) with the $K_m$ of complex I for artificial decylQ higher still (~140 mM) (34). Therefore, the lack of oxidation of $MitoQ_{10}$ by complex III (Fig. 2) is consistent with the $TPP^+$ moiety inhibiting penetration of the ubiquinone group into the hydrophobic environment surrounding the ubiquinone-binding sites of this enzyme.

In summary, here we have shown that the favored orientation of $MitoQ_{10}$ is with the $TPP^+$ moiety near the membrane surface and the ubiquinone penetrating into the membrane core (Figs. 3 and 4). This orientation enables the ubiquinone moiety to access the membrane core to act as a chain breaking antioxidant and allows recycling of $MitoQ_{10}$ to its ubiquinol form via reduction by complex II. In contrast $MitoQ_{10}$ cannot be oxidized by complex III explaining why it does not function as an electron carrier in mitochondrial respiration (3). These findings have significant implications for our understanding of the mode of action of mitochondria-targeted ubiquinones and will allow the rational optimization of other mitochondria-targeted molecules.

*Acknowledgments—We thank Edmund Kunji and Alex Hellawell for assistance with the electron microscopy and Michael Runswick and Martin Montgomery for assistance with isolation of complex II.*

## REFERENCES


1. Kelso, G. F., Porteous, C. M., Coulter, C. V., Hughes, G., Porteous, W. K., Ledgerwood, E. C., Smith, R. A., and Murphy, M. P. (2001) *J. Biol. Chem.* **276,** 4588–4596
2. Asin-Cayuela, J., Manas, A. R., James, A. M., Smith, R. A., and Murphy, M. P. (2004) *FEBS Lett.* **571,** 9–16
3. James, A. M., Cocheme, H. M., Smith, R. A., and Murphy, M. P. (2005) *J. Biol. Chem.* **280,** 21295–21312
4. Jauslin, M. L., Meier, T., Smith, R. A., and Murphy, M. P. (2003) *Faseb J.* **17,** 1972–1974
5. Adlam, V. J., Harrison, J. C., Porteous, C. M., James, A. M., Smith, R. A., Murphy, M. P., and Sammut, I. A. (2005) *Faseb J.* **19,** 1088–1095
6. Ng, Y., Barhoumi, R., Tjalkens, R. B., Fan, Y. Y., Kolar, S., Wang, N., Lupton, J. R., and Chapkin, R. S. (2005) *Carcinogenesis* **26,** 1914–1921
7. Murphy, M. P., and Smith, R. A. (2007) *Annu. Rev. Pharmacol. Toxicol.* **47,** 629–656
8. Ross, M. F., Kelso, G. F., Blaikie, F. H., James, A. M., Cocheme, H. M., Filipovska, A., Da Ros, T., Hurd, T. R., Smith, R. A., and Murphy, M. P. (2005) *Biochemistry (Mosc.)* **70,** 222–230
9. Liberman, E. A., and Topaly, V. P. (1969) *Biofizika* **14,** 452–461
10. Liberman, E. A., Topaly, V. P., Tsofina, L. M., Jasaitis, A. A., and Skulachev, V. P. (1969) *Nature* **222,** 1076–1078
11. Ketterer, B., Neumcke, B., and Laeuger, P. (1971) *J. Membr. Biol.* **5,** 225–245
12. Flewelling, R. F., and Hubbell, W. L. (1986) *Biophys. J.* **49,** 531–540
13. Flewelling, R. F., and Hubbell, W. L. (1986) *Biophys. J.* **49,** 541–552
14. Blatt, E., and Sawyer, W. H. (1985) *Biochim. Biophys. Acta* **822,** 43–62
15. Simkovic, M., and Frerman, F. E. (2004) *Biochem. J.* **378,** 633–640
16. Smith, A. L. (1967) *Methods Enzymol.* **10,** 81–86
17. Walker, J. E., Skehel, J. M., and Buchanan, S. K. (1995) *Methods Enzymol.* **260,** 14–34
18. Watmough, N. J., Loehr, J. P., Drake, S. K., and Frerman, F. E. (1991) *Biochemistry* **30,** 1317–1323
19. Griffin, K. J., Degala, G. D., Eisenreich, W., Muller, F., Bacher, A., and Frerman, F. E. (1998) *Eur. J. Biochem.* **255,** 125–132
20. DuPlessis, E. R., Pellett, J., Stankovich, M. T., and Thorpe, C. (1998) *Biochemistry* **37,** 10469–10477
21. Sharpley, M. S., Shannon, R. J., Draghi, F., and Hirst, J. (2006) *Biochemistry* **45,** 241–248

22. Ramsay, R. R., Steenkamp, D. J., and Husain, M. (1987) *Biochem. J.* **241,** 883–892
23. Darley-Usmar, V. M., Capaldi, R. A., Takamiya, S., Millett, F., Wilson, M. T., Malatesta, F., and Sarti, P. (1987) in *Mitochondria, A Practical Approach* (Darley-Usmar, V. M., Rickwood, D., and Wilson, M. T., eds), pp. 143–144, Oxford University Press, Oxford
24. Zhang, J., Frerman, F. E., and Kim, J. J. (2006) *Proc. Natl. Acad. Sci. U. S. A.* **103,** 16212–16217
25. Sazanov, L. A., and Hinchliffe, P. (2006) *Science* **311,** 1430–1436
26. Abrams, F. S., and London, E. (1993) *Biochemistry* **32,** 10826–10831
27. Wiener, M. C., and White, S. H. (1992) *Biophys. J.* **61,** 434–447
28. Tristram-Nagle, S., and Nagle, J. F. (2004) *Chem. Phys. Lipids* **127,** 3–14
29. Daum, G. (1985) *Biochim. Biophys. Acta* **822,** 1–42
30. Koehorst, R. B., Spruijt, R. B., Vergeldt, F. J., and Hemminga, M. A. (2004) *Biophys. J.* **87,** 1445–1455
31. Grinius, L. L., Jasaitis, A. A., Kadziauskas, Y. P., Liberman, E. A., Skulachev, V. P., Topali, V. P., Tsofina, L. M., and Vladimirova, M. A. (1970) *Biochim. Biophys. Acta* **216,** 1–12
32. Davey, G. P., Tipton, K. F., and Murphy, M. P. (1992) *Biochem. J.* **288,** 439–443
33. Lester, R. L., and Crane, F. L. (1959) *J. Biol. Chem.* **234,** 2169–2175
34. Lenaz, G. (1998) *Biochim. Biophys. Acta* **1364,** 207–221
35. Estornell, E., Fato, R., Castelluccio, C., Cavazzoni, M., Parenti Castelli, G., and Lenaz, G. (1992) *FEBS Lett.* **311,** 107–109
36. Rauchova, H., Fato, R., Drahota, Z., and Lenaz, G. (1997) *Arch Biochem. Biophys.* **344,** 235–241
37. Sun, F., Huo, X., Zhai, Y., Wang, A., Xu, J., Su, D., Bartlam, M., and Rao, Z. (2005) *Cell* **121,** 1043–1057
38. Gao, X., Wen, X., Esser, L., Quinn, B., Yu, L., Yu, C. A., and Xia, D. (2003) *Biochemistry* **42,** 9067–9080

# Interaction of the Mitochondria-targeted Antioxidant MitoQ with Phospholipid Bilayers and Ubiquinone Oxidoreductases

Andrew M. James, Mark S. Sharpley, Abdul-Rahman B. Manas, Frank E. Frerman, Judy Hirst, Robin A. J. Smith and Michael P. Murphy

*J. Biol. Chem. 2007, 282:14708-14718.*
*doi: 10.1074/jbc.M611463200 originally published online March 16, 2007*

---